



# Multi-phase transformation model of water quality in the sluice-controlled river reaches of Shayinghe River in China

Ming Dou<sup>1</sup> · Yaxin Cao<sup>1</sup> · Qingbin Mi<sup>2</sup> · Guiqiu Li<sup>1</sup> · Yanyan Wang<sup>1</sup>

Received: 20 June 2017 / Accepted: 10 December 2017 / Published online: 19 December 2017  
© Springer-Verlag GmbH Germany, part of Springer Nature 2017

## Abstract

To better understand the complex transformation mechanisms of pollutants in different phases in sluice-controlled river reaches (SCRs), a multi-phase transformation model of water quality is proposed. This model mainly describes the interactions of the water body, suspended matter, deposited sediments, and organisms. Mathematical expressions were first derived to describe the mass transportation processes in different phases of the river system. The multi-phase transformation model in SCRs was then established with defined physical mechanisms. Monitored data from the operation of Huaidian sluice were used to identify and validate the parameters of the transformation model and to simulate the spatial and temporal changes of pollutants in different phases. Four findings were made from the results. Firstly, the concentration values of pollutants in each phase in the upper and lower river reaches of the sluice are affected by flow, mode of sluice operation, and algal growth and enrichment. Secondly, the reaction processes in the upper and lower river reaches of the sluice indicate different dominant mechanisms according to the change in sluice operation. Thirdly, sluice operation leads to stronger exchanges between the water body and external materials because of the increased water disturbance. Fourthly, in the early period of the experiment, changes in the alga concentrations were mainly affected by water movement. In the later period, changes in the alga concentrations were mainly affected by the obstruction of the sluice in the upstream section, while these were affected by flow velocity, flow volume, and changes in nutrient concentration in the downstream section.

**Keywords** Water quality · Sluice-controlled river reaches · Transformation in different phases · Modeling · Shayinghe River

## Introduction

The sluice is a low-head hydraulic structure with the function of controlling and altering the natural flow of water to accommodate human needs by the operation of water resource managers. It is an important control engineering in water conservation systems constructed in rivers, reservoirs, lakes, and coastal areas for water retention and release, which has become one of the primary means of maintaining water supply, scientific management, and flood mitigation. Based on this,

they have been extensively applied in water supply networks, flood control, shipping, power generation, and irrigation. The construction of sluices has promoted the continuous development of industrial and agricultural productions in China, which is beneficial to the national economy. China has accumulated a wealth of engineering expertise in sluice construction. In recent years, the number of sluices in China has greatly expanded. For example, 5427 sluices are constructed in the Huaihe River basin, among which more than 600 are large or medium in size.

The effects of sluices on the river have attracted the attention of some scholars. The construction of sluices interrupts river continuity and blocks exchange of river material between the upper and lower reaches of the sluice. The river is restricted artificially, and the hydrological regime is altered significantly, such as reduced flow rate and hydrograph flashiness, which decreases the sediment transport capacity of the river (Zhang et al. 2015b). Furthermore, a sluice keeps water in the upper reaches of the dam, and the storage time of that water directly affects the water quality in the reservoir. For

Responsible editor: Marcus Schulz

✉ Ming Dou  
dou\_ming@163.com

<sup>1</sup> College of Water Conservancy and Environment, Zhengzhou University, No. 100 Kexue Road, Zhengzhou, Henan 450001, China

<sup>2</sup> Zhengzhou University Research Institute of Industrial Technology Co., Ltd, Zhengzhou 450000, China

most dams, the sluice gates are closed to store water during the dry season, which may lead to accumulation of highly concentrated pollution. Accordingly, sudden water pollution events may occur with flood discharge during the flood season. To some extent, sluice operation models have important effects on water quality.

Based on analysis of the temporal and spatial variations of hydrological factors and environmental indices, the literature indicated that construction and operation of sluices have great influences on the aquatic environment (Hu et al. 2008; Koutsos et al. 2010; Li et al. 2012; Gilmar and Marcos 2013; Liu et al. 2016; Chris et al. 2016). Many studies on sluices have focused on sediment deposition patterns and sedimentation rates, with the aim of reducing sedimentation and minimizing the impact on environment (Walling and Fang 2003; Kondolf et al. 2014; Petkovsek and Roca 2014; Wang et al. 2016b). Because of sediment resuspension, sluice operation can affect the concentration of suspended matter (Lothar and Klaus 2008; Enner et al. 2016; Frémion et al. 2016). Disturbance of sediments can lead to changes of pollutant concentration (e.g., organic compounds, total phosphorus, and total nitrogen) in downstream suspended sediment, and this will cause observed variation in the concentration of nutrients in the water body (Cui et al. 2011; Molisani et al. 2013). Changes in water temperature and aquatic ecosystems have association with sluice and dam regulation (Hakanson and Bryhn 2008; Zhang et al. 2016; Michalski et al. 2016). Influence factors on the water quality in sluice-controlled river reaches have been identified (Dou et al. 2013; Zhang et al. 2015a).

Because of increased public concern about water contamination in sluice-controlled river reaches (SCRs), a variety of hydrodynamic models and water quality models with pollutant transformation have been proposed in recent years to evaluate the influence of these structures on the environment. The Saint-Venant equations are applied in many hydrodynamic models as the basic control equations of river flow, and a great number of models are also developed in different conditions (Mevlut et al. 2009; Ludovic and Gilles 2012; Wang et al. 2013). In terms of water quality models, Hoff and Mackay (1993) first proposed a multi-media fugacity model to study the behavior and transformation of hazardous chemicals in a multi-media environment of air, water, sediment, suspended soil, and organisms, which characterize the paradigm of research on the transformation of pollutants in different phases. Some studies have investigated conceptual models including transformation processes of different forms of N and C nutrients (Liu et al. 2003; Chen et al. 2007; Guan et al. 2009; Wang et al. 2016a). In order to investigate the interactions of water body with respect to pollutant concentration, transformation models were established to simulate the migration and transformation processes of heavy metal pollutants, nonmetal inorganic pollutants, and organic pollutants (Lebo and Sharp

1992; Yang et al. 2012; Ao et al. 2016). There are also pollutant transformation models in the suspended matters and sediment matters (Tappin et al. 2003; Wang et al. 2015) and in the sediment matters and organisms (Hu and Li 2009; Li et al. 2014). General coupling models of the water quality and water quantity in rivers were developed to simulate hydrodynamic and water quality processes, such as the EFDC, MIKE, Water Quality Analysis Simulation Program (WASP), QUAL2K, and RMA4 models.

Overall, many researches are focused on the influence of sluice construction and operation on the water body in SCRrs. A series of hydrodynamic and water quality models have been created to simulate changes in water level, flow, and water quality. However, few studies have been conducted to investigate transformation processes of pollutants among the water body, suspended solids, sediments, and organisms.

Therefore, we developed a water quality model with all these four components of the river system. This model was used to simulate changes in water quality under different conditions of sluice operation. Experiments were carried out in the Huaidian sluice of Shayinghe River, China. The aim of this work is to explore the spatial and temporal characteristics and variations of pollutants during sluice operation. The results can be used to provide technical guidance for sluice operation.

## Materials and methods

### Study area

With the high density of population and high industrial and agricultural productions in Huaihe River basin, a lot of domestic sewage and industrial wastewater had been discharged into these rivers of the Huaihe River basin and the Shaying River is the largest and most polluted tributary of Huaihe River. The total amount of wastewater and pollutants accounts for more than 40% of the Huaihe River system, so it is known as the good or bad “barometer” of Huaihe River water quality, and the current serious pollution has become the highest priority in the work of water pollution prevention and control.

As the important control engineering of the main stream in Shaying River, the Huaidian sluice plays a key role in controlling upstream pollution for a long time and it is also one of the key sluice for the joint control of the Huaihe River pollution. The sources of pollutants in the Huaidian sluice are mainly domestic sewage, industrial wastewater, and agricultural fertilization, according to the monitoring data of Huaidian sluice, and the main pollutants are chemical oxygen demand (COD) and ammonia nitrogen. As the water quality is worse than the class IV level (Table 1) sometimes, water pollutants are more prominent and have drawn more and more attention in recent years (Xi et al. 2014; Chen et al. 2016; Hao et al. 2014, etc).

**Table 1** The pollutant-monitoring data of Huaidian sluice from 2003 to 2012 (mg/l)

Pollutants index	2003	2004	2005	2006	2007	2008	2009	2010	2011	2012
NH <sub>3</sub> -N	13.1	5.1	5.2	5.5	4.8	3.2	3.1	1.8	1.3	2.0
COD	17.7	8.8	7.1	7.3	7.2	6.4	6.1	5.1	6.2	9.2
TP	1.2	0.4	0.3	0.5	0.4	0.3	0.3	0.2	–	0.3

– this year lacks monitoring data

## Data collection

In order to study the effects of sluice operation on the transformation process of pollutants in different phases, the Huaidian sluice was taken as an example, and three experiment schemes of sluice operation were carried out. The experiment was within the scope of 2 km upstream and downstream in sluice-controlled river reaches. The first upstream section was 850 m away from Huaidian sluice, and the last section downstream was 1150 m away from Huaidian sluice. In the research river, seven sections were set and the interval distance between the adjacent sections was 200–500 m. There were no sewages in the experimental area. The layout diagram of monitoring sampling sections and sampling points is shown in Fig. 1.

Combined with three experiment results carried out on March 2013, the research mainly focused on the water quality transformation rules among different carriers, such as water, suspended matters, and sediments, under different operation models. Five monitoring sections (sections I, III, and IV in the upper reaches of the sluice; sections VI and VII in the lower reaches of the sluice) were set in the experiment, and systemic sampling was conducted 7 times, including 18 water samples, 3 sediment samples, and 4 upper-cover water samples, to detect the suspended pollutant concentration. The water quality was monitored by the water quality-monitoring module of HACH and alga automatic monitor of DS5 in the upper and lower reaches of the sluice. Considering the sluice operation effects on pollutant transformation in different phases during the entire experiment period, six opening modes of sluice gate were designed (30 cm of 8 holes, 50 cm of 6 holes, 70 cm of 4 holes, 30 cm of 4 holes, 10 cm of 4 holes, all holes closed). The specific experiment detection process and monitoring values of water level, water flow, and water velocity in the initial section are described in Table 2.

## Transformation processes of pollutants in different phases

The construction of sluices changes the river hydrological conditions, which may lead to the change of hydrodynamic conditions in the SCRRs, such as changes in water level, flow velocity, sediment-carrying capacity, and sediment-settling velocity. These changes further influence the transformation processes of pollutants associated with different media,

including water, suspended matter, and sediment. The driving effects of water quality transformation may differ, even for the same transformation process, because of the changes in sluice regulation, which may lead to differences in concentration of pollutants in different media.

For example, the natural flow of a river is obstructed and the original continuity is destroyed when a sluice is closed. At this time, the river in the upper reaches of the sluice is similar to a reservoir, and the flow velocity in this area is slower than it would be in the natural river reach. Therefore, the adsorption and sedimentation of suspended particles in the water body are significant in this area, leading to the retention of a large amount of sediment and nutrients in the upper reaches of the sluice. At the same time, large amounts of dissolved pollutants are absorbed by suspended particles and settled to the bottom of the river, where they are degraded or consolidated. The increased water depth in front of the sluice also causes temperature stratification in the water body, which dramatically changes the living environment of aquatic organisms. However, the lower reaches of the sluice are similar to a dead lake water without water supplementation, and water bloom phenomena may occur because of increased nutrient concentrations with long-term evaporation.

When the sluice is opened, the scouring effect of water flow at the riverbed is strengthened and the migration and transformation processes associated with pollutants also change as the hydrodynamic conditions change in the SCRRs. At this point, water reaeration is enhanced because of the increase in flow velocity, which further causes an increase in the aerobic respiration of organisms and water self-purification capacity. The resuspension of pollutants in sediment is strengthened by the agitation of the discharged flow in front of the sluice. The pollutant particles are decomposed and redissolved in baffle-wall style in the lower reaches of the sluice, which results in a decrease in suspended and dissolved pollutant concentrations. The bioaccumulation of organisms is reduced due to the environment in which the accumulation of algae and bacteria is disturbed by the change of hydrodynamic conditions. The transformation processes of pollutants in different phases in the SCRRs are shown in Fig. 2.

To describe these complex transformations of pollutant in different phases in the SCRRs, a mathematical model was developed with two characteristics. The one is that the model highlights the hydrodynamic effects of river disturbance with sluice gate operation, specifically the numerical calculation

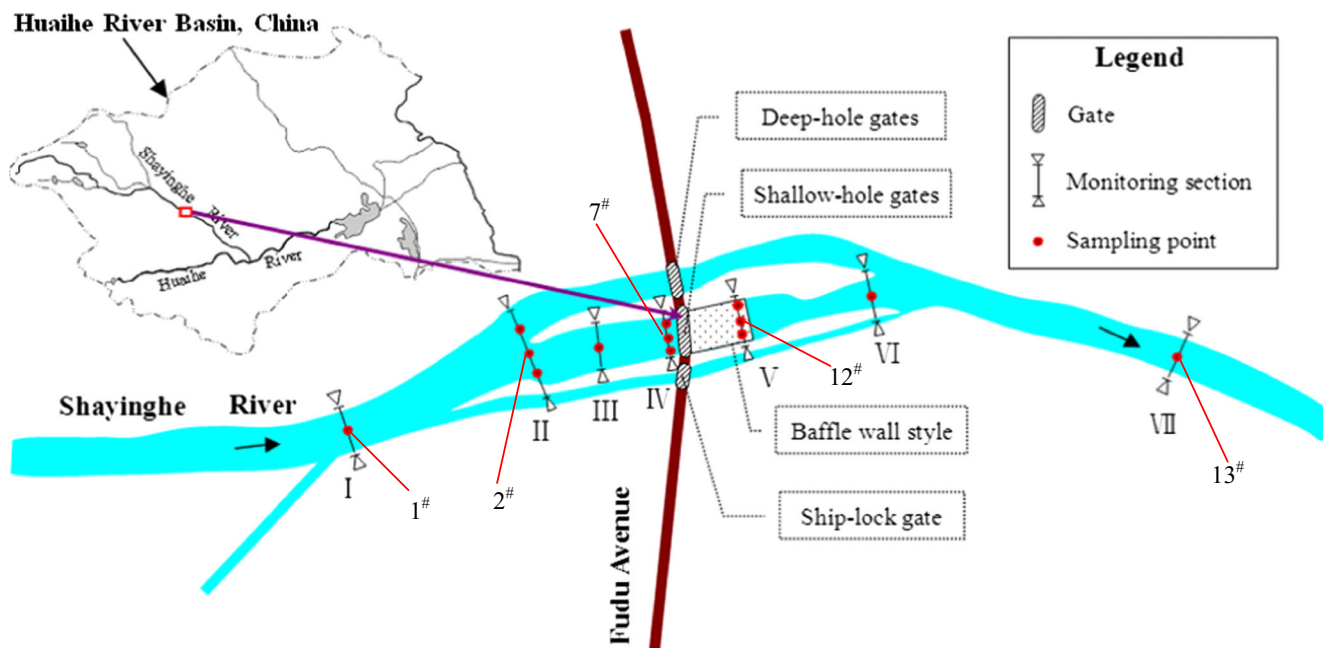


Fig. 1 Sketch of river reaches near the Huaidian sluice during the experiments

for the section of the sluice gate and other unconventional river section. The other is that the model describes the transformation of pollutants in different phases accurately and comprehensively, including migration and transformation processes, adsorption and desorption processes of the dissolved and suspended pollutants, sedimentation and resuspension processes of the suspended and deposited sediment pollutants, and biological intake and endogenous respiration processes.

**Hydrodynamic model incorporating sluice operation**

Being obstructed and restricted by the sluice gate, the flow process of SCRRs is more complicated than that in the open channel. A hydrodynamic model was used to calculate hydrodynamic parameters such as water level, flow volume, and velocity in SCRRs. In order to effectively reflect the current character of SCRRs, the model considers different conditions, combining with the topographic features.

For the reaches without sluices, the hydrodynamic model can be expressed by the two-dimensional Saint-Venant equations (Eqs. 1, 2, and 3):

$$\frac{\partial z}{\partial t} + \frac{\partial q_x}{\partial x} + \frac{\partial q_y}{\partial y} = 0 \tag{1}$$

$$\frac{\partial q_x}{\partial t} + \frac{q_x}{h} \frac{\partial q_x}{\partial x} + \frac{q_y}{h} \frac{\partial q_x}{\partial y} + gh \frac{\partial z}{\partial x} + g \frac{n^2 q_x \sqrt{q_x^2 + q_y^2}}{h^{7/3}} = 0 \tag{2}$$

$$\frac{\partial q_y}{\partial t} + \frac{q_x}{h} \frac{\partial q_y}{\partial x} + \frac{q_y}{h} \frac{\partial q_y}{\partial y} + gh \frac{\partial z}{\partial y} + g \frac{n^2 q_y \sqrt{q_x^2 + q_y^2}}{h^{7/3}} = 0 \tag{3}$$

where  $z$  is the water level;  $h$  is the mean flow depth;  $q_x$  and  $q_y$  are the specific discharges in the  $x$  and  $y$  directions, respectively;  $g$  is the acceleration of gravity; and  $n$  is the roughness coefficient.

For the reaches with sluices, it is hard to directly calculate the water discharge through sluices by the Saint-Venant

Table 2 Design of the regulation experiment of the Huaidian sluice

Time	Regulation modes	Sampling position		
		Water samples	Suspended particle samples	Sediment samples
16:30 Mar. 5	8 holes, 30 cm	1#, 7#, 12#, 13#	2#, 7#	1#, 7#, 13#
09:00 Mar. 6	6 holes, 50 cm	1#, 7#, 12#, 13#		
15:00 Mar. 6	6 holes, 50 cm	1#, 7#, 12#, 13#	2#, 7#	
09:30 Mar. 7	4 holes, 70 cm	1#, 7#, 12#, 13#		
13:30 Mar. 7	4 holes, 70 cm	1#, 7#, 12#, 13#	2#, 7#	
08:30 Mar. 8	4 holes, 10 cm	1#, 7#, 12#, 13#		
12:30 Mar. 8	All holes closed	1#, 7#, 12#, 13#	2#, 7#	

# refers to the sampling point

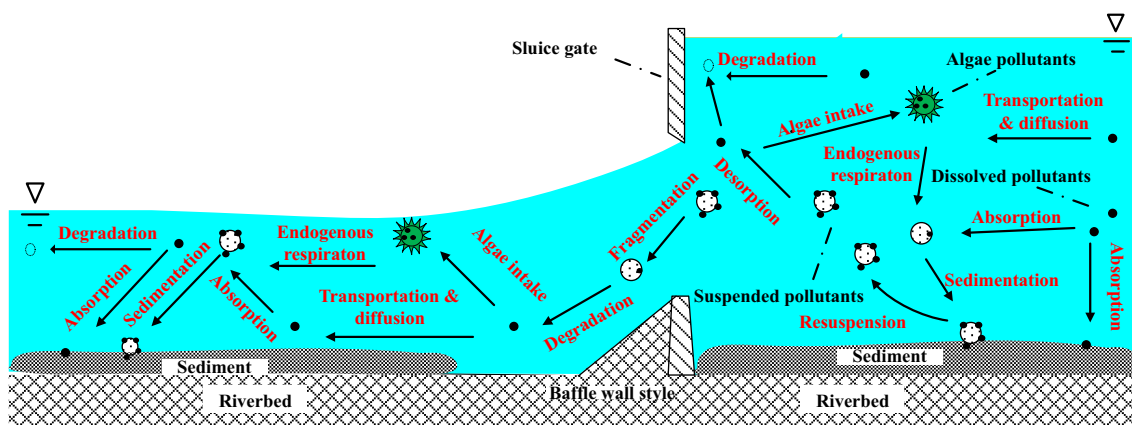


Fig. 2 Conceptual map of the transformation of pollutants in different phases in the sluice-controlled river reaches

equations due to the constraint of gates on water flow. Therefore, an improved bidirectional iterative internal boundary control method is implemented to address the internal boundary (Dou et al. 2015).

The free outflow or submerged outflow can be expressed as follows:

$$q = \sigma_s \mu B e \sqrt{2gh_a} \tag{4}$$

where  $q$  is the water discharge through the sluice and  $\sigma_s$  is the submergence coefficient that is related to the upstream and downstream water depths and the gate opening size. When  $\sigma_s = 1$ , the water undergoes free flow; when  $0 < \sigma_s < 1$ , there is submerged outflow.  $\mu$  is the discharge coefficient,  $e$  is the gate opening size,  $B$  is the width of the sluice gate, and  $h_a$  is the mean water depth in front of the sluice.

The flow continuity equation can be expressed as follows:

$$q_a^j = q_b^j = q \tag{5}$$

where  $q_a^j$  and  $q_b^j$  are the water discharges in front of the sluice and behind the sluice, respectively, at the  $j$ th time step.

### Transformation model of pollutants in different phases

A transformation model of pollutants in different phases was developed to describe the physical, chemical, and biological processes of pollutant concentration in different media, such as water, suspended matter, deposited sediment, and aquatic organisms, and to represent the temporal and spatial changes of pollutants in these different phases. This model included seven indices: algae (PYT), COD, dissolved oxygen (DO), ammonia nitrogen (NH<sub>3</sub>-N), nitrate nitrogen (NO<sub>3</sub>-N), organic nitrogen (ON), and total phosphorus (TP). To represent the transformation processes, three indices (i.e., COD, ON, and TP) were chosen to reflect the transformation of the dissolved, suspended, and sedimented pollutants; the other indices were only

considered for the dissolved pollutants. The reaction processes of them are shown in Fig. 3.

The transformation model of pollutants in different phases was constructed with four equations: a fundamental equation of water quality transport and transformation, an equation of adsorption–desorption reactions, an equation of sedimentation–resuspension reactions, and a kinetic equation of algal growth. The fundamental equation reflects the transformation of contaminant concentration in each phase, and the other equations describe the physical mechanisms of pollutant mass transfer in different phases.

### Fundamental equations of pollutant transport and transformation

The fundamental equations include the fundamental items and the transformation items. The former describes the transport and diffusion processes of water, and the latter describes the mass transformation processes in different phases.

The fundamental equation of the dissolved pollutant concentrations is given as follows:

$$\begin{aligned} \frac{\partial C_d}{\partial t} + u \frac{\partial C_d}{\partial x} + v \frac{\partial C_d}{\partial y} - E_x \frac{\partial^2 C_d}{\partial x^2} + E_y \frac{\partial^2 C_d}{\partial y^2} \\ = N'_{bd} - N_{dw} - N_{db} - N_{de} + N'_{ed} - N_1 \end{aligned} \tag{6}$$

where  $C_d$  is the concentration of dissolved pollutants;  $u$  and  $v$  are the flow velocity components in the  $x$  and  $y$  directions;  $E_x$  and  $E_y$  are the diffusion coefficient components in the  $x$  and  $y$  directions;  $N'_{bd}$  is the transform flux from sediment pollutants to dissolved pollutants through desorption;  $N_{dw}$  is the transform flux from dissolved pollutants to suspended pollutants by adsorption;  $N_{db}$  is the transform flux from dissolved pollutants to sediment pollutants by adsorption;  $N_{de}$  is the loss of flux of the dissolved pollutants by aquatic organism intake;  $N'_{ed}$  is the increasing flux of the dissolved pollutants caused by endogenous

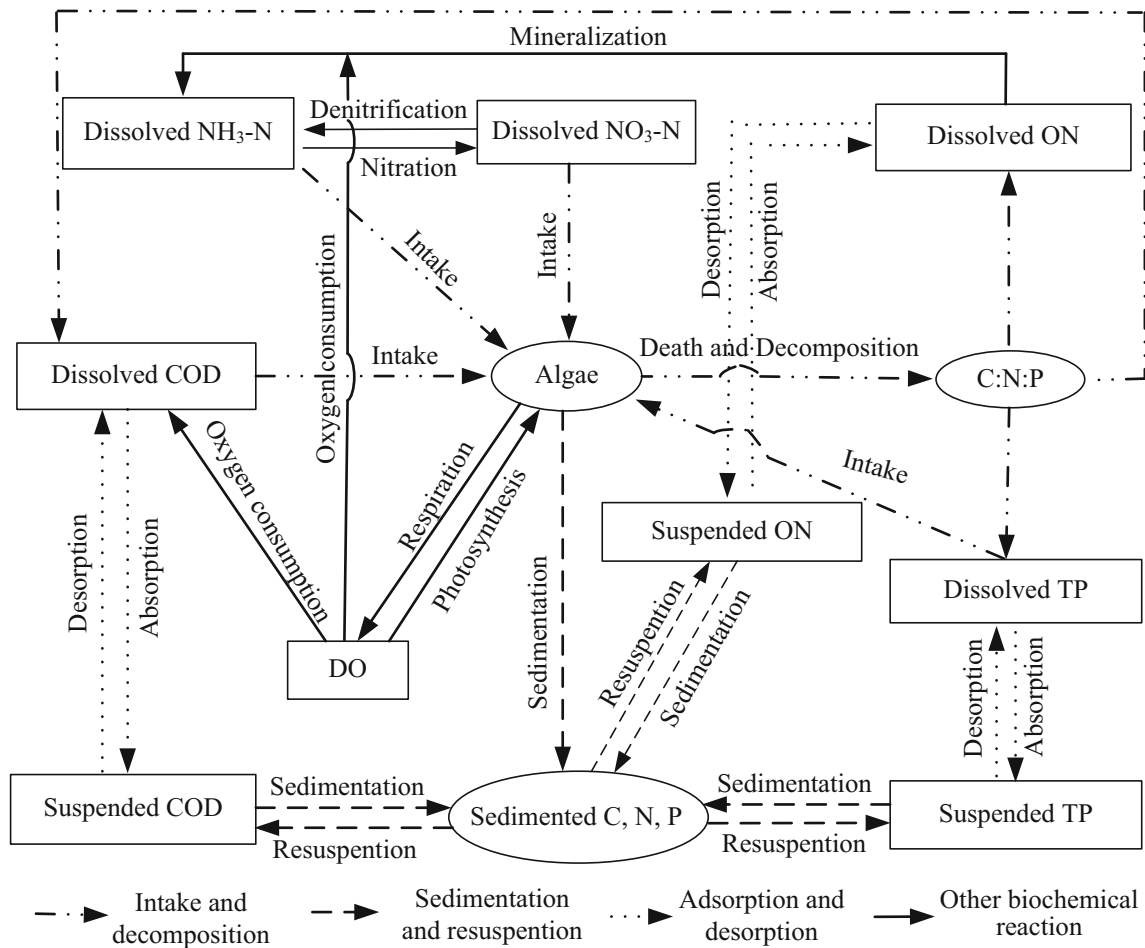


Fig. 3 Schematic diagram of the transformation of pollutants in different phases

respiration and death of aquatic organisms;  $N_1$  is the loss of flux of the dissolved pollutants caused by other biochemical reactions; and  $N_1 = K_1 C_d$ , where  $K_1$  is the degradation coefficient of the dissolved pollutants.

The fundamental equation of the suspended pollutant concentration is given as follows:

$$\frac{\partial C_w}{\partial t} + u \frac{\partial C_w}{\partial x} + v \frac{\partial C_w}{\partial y} - E_x \frac{\partial^2 C_w}{\partial x^2} + E_y \frac{\partial^2 C_w}{\partial y^2} = N_{dw} + N_{bw} - N'_{wb} - N_2 \tag{7}$$

where  $C_w$  is the concentration of suspended pollutants;  $N_{bw}$  is the transform flux from the sediment pollutants to the suspended pollutants through resuspension;  $N'_{wb}$  is the transform flux from the suspended pollutants to the sediment pollutants caused by sedimentation;  $N_2$  is the loss of flux of the suspended pollutants caused by other biochemical reactions; and  $N_2 = K_2 C_w$ , where  $K_2$  is the degradation coefficient of the suspended pollutants.

The fundamental equation of sediment pollutant concentration is given as follows:

$$\frac{\partial C_b}{\partial t} + u_b \frac{\partial C_b}{\partial x} + v_b \frac{\partial C_b}{\partial y} = N'_{wb} + N_{eb} + N_{db} - N_{bw} - N'_{bd} - N_3 \tag{8}$$

where  $C_b$  is the concentration of sediment pollutants; its unit is different from that of the dissolved pollutants. Based on the method of monitoring pollutants in the sediment, this variable represents weight per square meter in the sediment;  $u_b$  and  $v_b$  are flow velocity components of sediment in the  $x$  and  $y$  directions (m/s), which are typically negligible because their values are much smaller than those of the water body;  $N_{eb}$  is the increasing flux of sediment pollutants caused by algal death and deposition;  $N_3$  is the loss of flux of sediment pollutants caused by other biochemical reactions; and  $N_3 = K_3 C_b$ , where  $K_3$  is the degradation coefficient of sediment pollutants.

### Adsorption and desorption equations

The contents of pollutants related to adsorption and desorption are represented in the fundamental equation, mainly including three parts: the adsorption flux  $N_{dw}$  of suspended particles of dissolved pollutants, the adsorption flux  $N_{dw}$  of dissolved pollutants in sediments, and the desorption flux  $N'_{bd}$  of the dissolved pollutants in sediments. Although the suspended pollutants also desorb under certain conditions, desorption processes are generally negligible. This is mainly because of the low concentration of suspended particles in the water body, resulting a smaller desorption effect than that of the sediments. To describe the transformation flux of adsorption and desorption, we assume that suspended particles are evenly distributed in the water and that the adsorption flux of the particles is proportional to the difference between the concentration of the pollutants in the particle surface solution and that in the water body. The adsorption flux of the suspended particles and sediments can be expressed as

$$N_{dw} = K_{xf1}(C_w - C_d) \tag{9}$$

$$N_{db} = K_{xf2}(C_b - C_d) \tag{10}$$

where  $K_{xf1}$  and  $K_{xf2}$  are the adsorption coefficients of the suspended particles and the dissolved pollutants in the sediments, respectively.

Desorption, which refers to the transformation of pollutant contents from the solid phase to the liquid phase, is the reverse process of adsorption. Therefore, desorption flux can be expressed as follows:

$$N'_{bd} = K_{jx}(C_b - C_d) \tag{11}$$

where  $K_{jx}$  is the desorption coefficient.

### Sedimentation and resuspension equations

The transformation of sediment pollutants significantly differs from that of the dissolved and suspended pollutants. Diffusion of sediment pollutants is insignificant because compounds are attached to the sediment particles at the river bottom and they are influenced mainly by the pushing action of water flow. The pollutants related to sedimentation and resuspension represented in the fundamental equation include two parts: One is the sedimentation flux  $N'_{wb}$  of the suspended pollutants; the other is the resuspension flux  $N_{bw}$  of the sedimented pollutants. Based on relevant principles of sediment dynamics, the sedimentation and resuspension of pollutants in the particle phase are related to the movement of suspended particles in the water body, which is closely related to the water flow conditions.

It has been demonstrated in practice that the sedimentation and resuspension of sediment particles in the water body

depend mainly on the critical flow velocity. If the actual flow velocity is lower than the critical flow velocity (in which case sedimentation is dominant), the transformation flux of suspended pollutants caused by sedimentation is expressed as follows:

$$N'_{wb} = K_w/HC_w \tag{12}$$

where  $K_w$  is the sedimentation rate of suspended pollutants and  $H$  is the water depth.

However, if the actual flow velocity is higher than the critical flow velocity (in which case resuspension is dominant), the transformation flux of sedimented pollutants from resuspension is expressed as follows:

$$N_{bw} = K_s/H \tag{13}$$

where  $K_s$  is the resuspension rate of sedimented pollutants.

### Algal growth kinetic equations

Biogenic substances in the water body, such as nitrogen, phosphorus, and carbon, can be absorbed by algae. Then, the algae will be decomposed into inorganic substances and sink to the riverbed after dying. Therefore, algal growth kinetics can be used to describe the conversion processes between algae and pollutants. The interaction of algal growth and pollutant concentration represented in the fundamental equation includes two parts: One is the intake flux  $N_{dw}$  of dissolved pollutants from algae; the other is the attenuation flux  $N_{eb}$  of sedimented pollutants from algae. These components can be expressed as follows:

$$N_{de} = G_p C_e \tag{14}$$

$$N_{eb} = \left( D_p + \frac{\omega_p}{H} \right) C_e + D_z Z(t) \tag{15}$$

where  $G_p$ ,  $D_p$ , and  $\omega_p$  are the alga growth rate, death rate, and sedimentation rate, respectively;  $D_z$  is the alga predation rate; and  $Z(t)$  is the biomass concentration of their predators.

The mechanism of algal growth kinetics in the aquatic environment can be described as follows:

$$G_p = G_{max} \times G_T \times G_I \times G_N \tag{16}$$

where  $G_{max}$  is the maximum growth rate of algae;  $G_T$ ,  $G_I$ , and  $G_N$  are the temperature regulation factor, light attenuation factor, and nutrient-limiting factor (dimensionless), respectively. The nutrient-limiting factor  $G_N$  is influenced by the concentrations of dissolved nitrogen and phosphorus, which can be expressed as follows:

$$G_N = \min \left( \frac{C_{dN}}{K_{mN} + C_{dN}}, \frac{C_{dP}}{K_{mP} + C_{dP}} \right) \tag{17}$$

where  $C_{dP}$  and  $C_{dN}$  are the concentration of dissolved inorganic nitrogen (DIN) and dissolved inorganic phosphorus (DIP), respectively, both of which are essential for growth of algae, and  $K_{mN}$  and  $K_{mP}$  are the Michaelis constants of DIN and DIP, respectively.

## Results and discussion

### Model verification

In terms of hydrodynamic boundary conditions, the flow monitor data from section I were used as upper boundary conditions, the water level data from section VII were used as lower boundary conditions, and the water level data from section IV were used as internal boundary conditions. The measured water level and water flow data were used as initial conditions. For the boundaries of the transformation model, the measured pollutant concentration data series of the dissolved pollutants from section I was used as the upper boundary conditions during this period. The dissolved, suspended, and sediment pollutant concentration data measured from the monitoring section were used as starting conditions during this period.

To verify the hydrodynamic model, the parameters of these models were calibrated using the data monitored at section III in the upper reaches of the sluice and verified using the data monitored at section VI in the lower reaches of the sluice. The simulation results showed that the maximum relative error for section IV was 11.63%, with an average relative error of 4.46%, and the maximum relative error for section VI in the lower reaches of the sluice was 9.79%, with an average relative error of 5.50%. Therefore, the simulation results were generally in good accordance with the measured data.

Considering that it is very complex to calibrate a single parameter with so many parameters in the model, parameter calibration for the transformation model of pollutants in different phases was performed as follows. Firstly, parameters were classified on basis of the degree of sensitivity of the model to each parameter. The sensitive parameters include stream reaeration coefficient ( $teta r$ ), adsorption coefficient ( $k_{xf}$ ), desorption coefficient ( $k_{jx}$ ), sedimentation rate of organic matter ( $k_w$ ), resuspension rate of organic matter ( $k_s$ ), mineralization rate ( $m_{lr}$ ), and denitrification rate ( $D_{fr}$ ). The insensitive parameters include the maximum photosynthetic oxygen production ( $P_{MAX}$ ), subsaturating oxygen concentrations ( $Cos$ ), Michaelis constant of nitrogen ( $K_{mN}$ ), and Michaelis constant of phosphorus ( $K_{mP}$ ). Secondly, partial suggested values of parameters derived from some environmental models (e.g., the MIKE ECO Lab and WASP models) and calibrated parameters reported in the literature (Xia et al. 2001) were used as initial model parameter values. Thirdly, the values of each sensitive parameter were adjusted constantly and the simulated result was compared with the measured

result for specified phases, meanwhile, to determine the value of each sensitive parameter. The insensitive parameters were maintained at their initial values. Finally, the sensitive parameters were taken together to simulate results by uniformly adjusting the parameter values.

The monitored data at section IV in the upper reaches of the sluice were used to calibrate the model parameters, and the monitored data at section VII in the lower reaches of the sluice were used to verify the model. Results showed that the maximum relative error at section IV in the upper reaches of the sluice was 35.5%, with an average relative error of 9.76%, and the maximum relative error at section VI in the lower reaches of the sluice was 63.75%, with an average relative error of 11.72%. Comparison of the results indicates that the simulated values of the model generally agree with the monitored data, and it can be used to simulate the transport processes of pollutants in different phases. The parameters of the transformation model of pollutants in different phases are shown in Table 3.

### Analysis of the simulation results

#### Simulation results and analysis of the dissolved pollutant concentrations

The changing patterns of dissolved pollutant concentrations in the upper and lower reaches of the sluice were simulated by the transformation model of pollutants described above for a period when the sluice was operated continuously (Fig. 4).

Figure 4 shows that the COD and ON concentrations generally decreased in the upper reaches of the sluice, whereas the TP concentration was irregular. In the lower reaches of the sluice, the COD concentration first decreased and then increased whereas ON presented the opposite trend and TP irregularly changed, reaching a maximum of 0.178 mg/l at 3:00 a.m. on March 6 and a minimum of 0.137 mg/l at 9:00 a.m. on March 7.

In consideration of large water flow in the earlier stage in the upper reaches of the sluice, COD and ON concentrations were diluted to an extent, which accelerated the mineralization of ON and led to a small decrease in ON concentration. The COD pollutant mainly existed in the dissolved phase, whereas a portion of the ON presented in the dissolved phase and another portion were transformed into ammonia nitrogen because of mineralization. The degradation and absorption of dissolved COD and ON accelerated with the decrease of gate opening size and flow velocity and the increase in water level in front of the sluice during the later stage. This finding demonstrated that suspended and sediment COD and ON increased because of decreased incoming water discharge, which caused a decrease in mineralization and increase in degradation and absorption. The dissolved TP concentration was mainly influenced by incoming water discharge and



**Table 3** Parameters of the transformation model of pollutants in different phases

Symbol	Meaning	Unit	Value	Symbol	Meaning	Unit	Value
$teta_r$	Stream reaeration coefficient	–	0.67	$C_{NH3-N}$	Subsaturating concentrations of $NH_3-N$	mg/l	0.05
$pro2$	Quantity of output of respiration	–	1	$D_{IRI}$	Denitrification rate	l/day	4
$P_{MAX}$	Maximum photosynthetic oxygen production	l/day	3.5	$M_{IRI}$	Mineralization rate	l/day	0.46
$Cos$	Subsaturating oxygen concentrations	mg/l	2	$K_w$	Sedimentation rate of organisms	m/day	0.1
$DP$	Phytoplankton mortality	l/day	0.099	$K_S$	Resuspension rate of organisms	$g/m^2/day$	1
$GP$	Phytoplankton growth rate	l/day	0.1	$U_{crit}$	Critical velocity	m/s	0.2
$CdN$	Nitrogen concentration of phytoplankton growth	mg/l	0.2	$N_{IDO}$	DO of nitrification	$g O_2/g NH_4$	4.47
$K_{mN}$	Michaelis constant of nitrogen	–	0.05	$K_I$	$K_{ICOD}$	Degradation coefficient of COD	l/day
$C_{dp}$	Phosphorus concentration of phytoplankton growth	mg/l	0.02	$K_{ION}$	Degradation coefficient of ON	l/day	0.25
$K_{mp}$	Michaelis constant of phosphorus	–	0.15	$K_{JKCOD}$	Desorption coefficient of COD	l/day	0.00015
$D_Z$	Prey rate of aquatic organisms	l/day	0.015	$K_{JKTP}$	Desorption coefficient of TP	l/day	0.00015
$G_{MAX}$	Maximum growth rate of phytoplankton growth	l/day	2.5	$K_{JKON}$	Desorption coefficient of ON	l/day	0.00046
$Z(t)$	Biomass concentration of predators	mg/l	0.24	$K_{JKCOD}$	Adsorption coefficient of COD	l/day	0.031
$AmpU$	$NH_3-N$ intake of plants	–	0.066	$K_{JKTP}$	Adsorption coefficient of TP	l/day	0.0001
$U_{COD}$	COD absorbed of plant growth	–	0.02	$K_{JKON}$	Adsorption coefficient of ON	l/day	0.00012
$U_{TP}$	Phosphorus requirement of photosynthesis	$g P/g O_2$	0.091	$N_{IRI}$	Attenuation of $NH_3-N$	l/day	1.54
$U_{NR}$	Nitrate requirement of photosynthesis	$g NO_3^-/g O_2$	0.066	$a_{NC}$	Ratio of nitrogen and carbon in algae	–	0.09
				$a_{PC}$	Ratio of phosphorus and carbon in algae	–	0.012

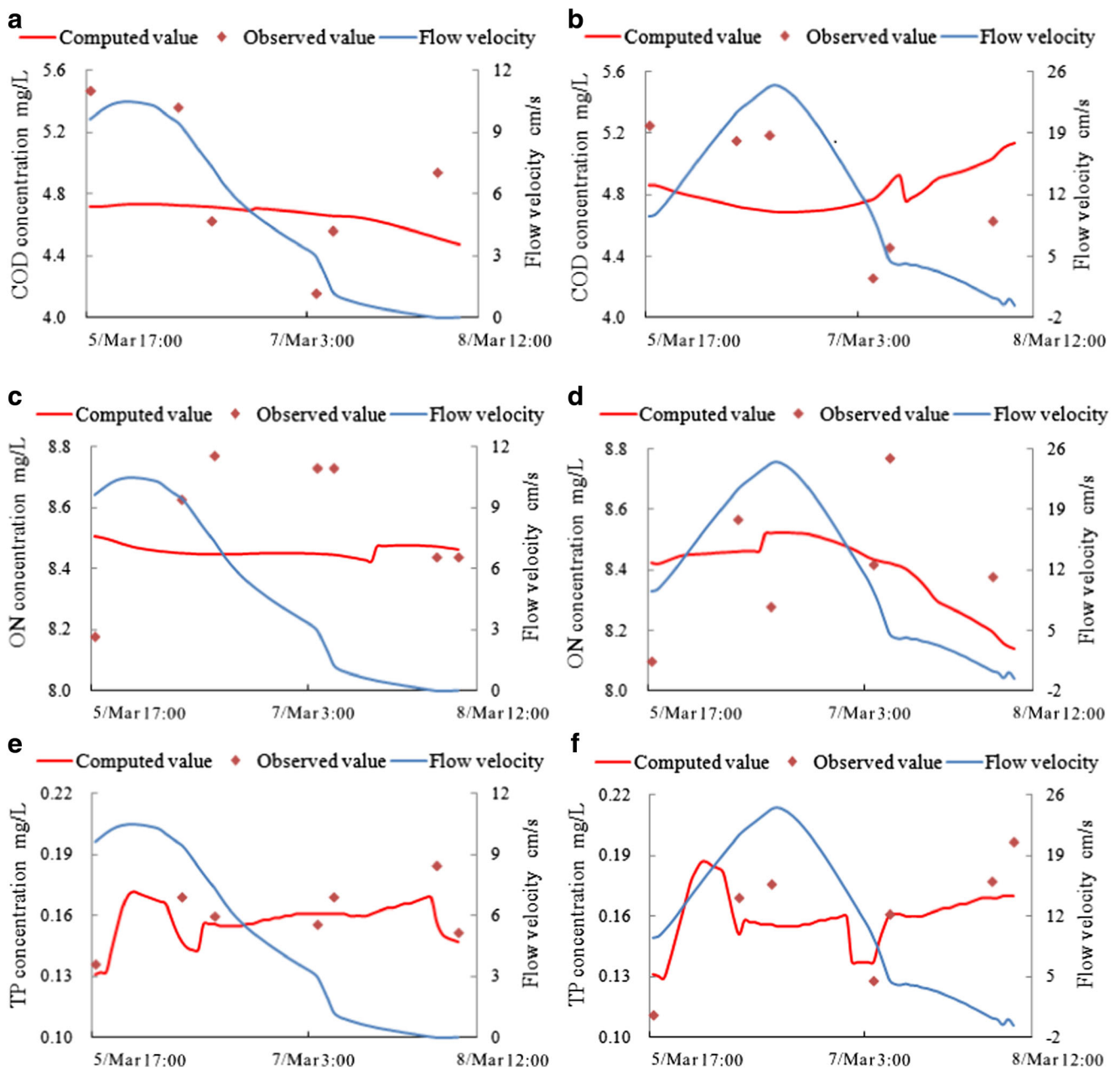


**Fig. 4** Trends of the concentrations of COD (a), ON (c), and TP (e) in the upper reaches of the sluice and the concentrations of COD (b), ON (d), and TP (f) in the lower reaches of the sluice of the dissolved pollutants

sluice operation mode. During the early period, the same correlation between TP concentration and flow velocity of the section indicated that the change of TP concentration was mainly affected by the water in the upstream. This relationship is caused by the decreases in the gate opening size and incoming water discharge, which caused increased adsorption and decreased desorption of dissolved TP. The release rate of phosphorus from other matter (e.g., BOD) in the water body was accelerated to an extent, which led to a slight increase in TP concentration. On 8:00 a.m. on March 8, the dissolved phosphorus, suspended phosphorus, and sediment

phosphorus concentrations began to decrease, and the TP concentration also began to decrease because of the closing of the sluice gates, which led to blocked water flow and a rise in the water level.

In the lower reaches of the sluice, the dissolved COD concentration was predicted to increase with the release of discharge from the sluice gate and this caused disturbances in the downstream water body. But the simulation curve showed a decrease, which indicated that desorption of sediment COD was not notable during this period. However, the quantity of algae increased rapidly around 11:00 a.m.

on March 6 and 4:00 p.m. on March 7. The COD concentration also decreased, which indicated that the photosynthetic carbon produced by algae around this time was insufficient for growth, and a portion of the carbon needed was absorbed from the water body. The amount of algae quantity decreased another time, and the COD concentration increased due to the decomposition of algae in water. Thus, COD was transformed mainly between the dissolved COD and biological COD in the earlier stage. The simulation results of dissolved ON concentration showed that the changes of the ON concentration and flow velocity were correlative. They first increased and then decreased. The reason of this relationship is that the discharge volume was greater when the gate opening size was larger, which led to relatively notable desorption of sediment ON and mineralization of dissolved ON. Nitrogen was mainly presented as ON and NH<sub>3</sub>-N during this period. With the decrease of sluice gate opening size, the discharge volume also gradually decreased. The dissolved ON decreased rapidly because it was gradually adsorbed into the suspended ON and sediment ON. It is clear that the dissolved ON concentration could be affected by the gate opening size of the sluice gate and mineralization. The pattern of the simulation results for dissolved TP concentration is complex. The TP concentration increased in the earlier stage because of the scour of the sediments caused by the discharge from the large opening. TP maintained a steady state in the middle stage, and this indicated that the self-degradation of the dissolved TP, desorption of the sediment, and absorption of algal growth reached a relative balance at this time. In the later stage, the gate opening size of the sluice and the scouring effect of the flow on the sediment decreased. The

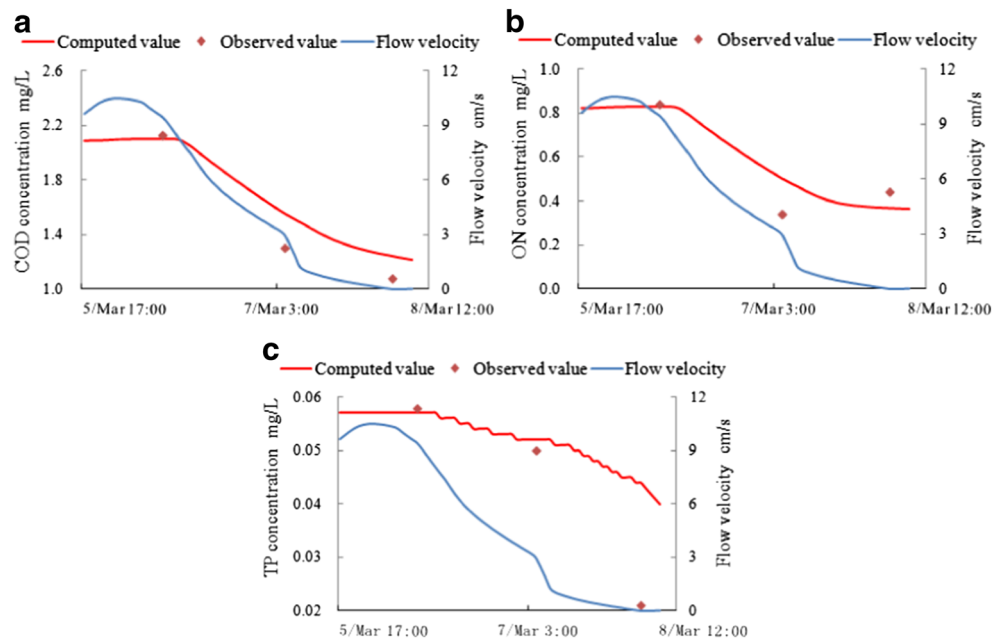
amount of algae first decreased and then increased, which indicated that the change of the TP concentration was mainly influenced by the decomposition of algae. Overall, change of the TP concentration would be reasonably influenced by hydrodynamic conditions and alga growth and death.

**Simulation results and analysis of the suspended pollutant concentrations**

Based on the design of the third experiment, four upper-cover water sampling points were chosen in section IV in the upper reaches of the sluice and corresponding simulation results of this section were analyzed. This comparison analysis is shown in Fig. 5.

Figure 5 shows that changes of the suspended COD, suspended TP, and suspended ON concentrations were approximately correlative with the flow velocity, which changed little in the earlier stage, rapidly decreased in the middle stage, and slowly decreased or maintained in the later stage. The parameter calibration also showed that the critical velocity (i.e., 0.2 m/s) was sensitive to TP and ON concentrations, but not very sensitive to other parameters. The simulation results of flow velocity in Fig. 5 indicated that sedimentation played a dominant role in the suspended pollutants in the upper reaches of the sluice during the entire experimental period. In the earlier stage, the flow velocity decreased because of the large incoming discharge in the initial section, and the flow velocity was lower than the critical velocity because of the blocking of the sluice gate when the flow reached the section near the sluice. However, changes of the pollutant concentrations

**Fig. 5** Trends of the concentrations of suspended COD (a), suspended ON (b), and suspended TP (c)



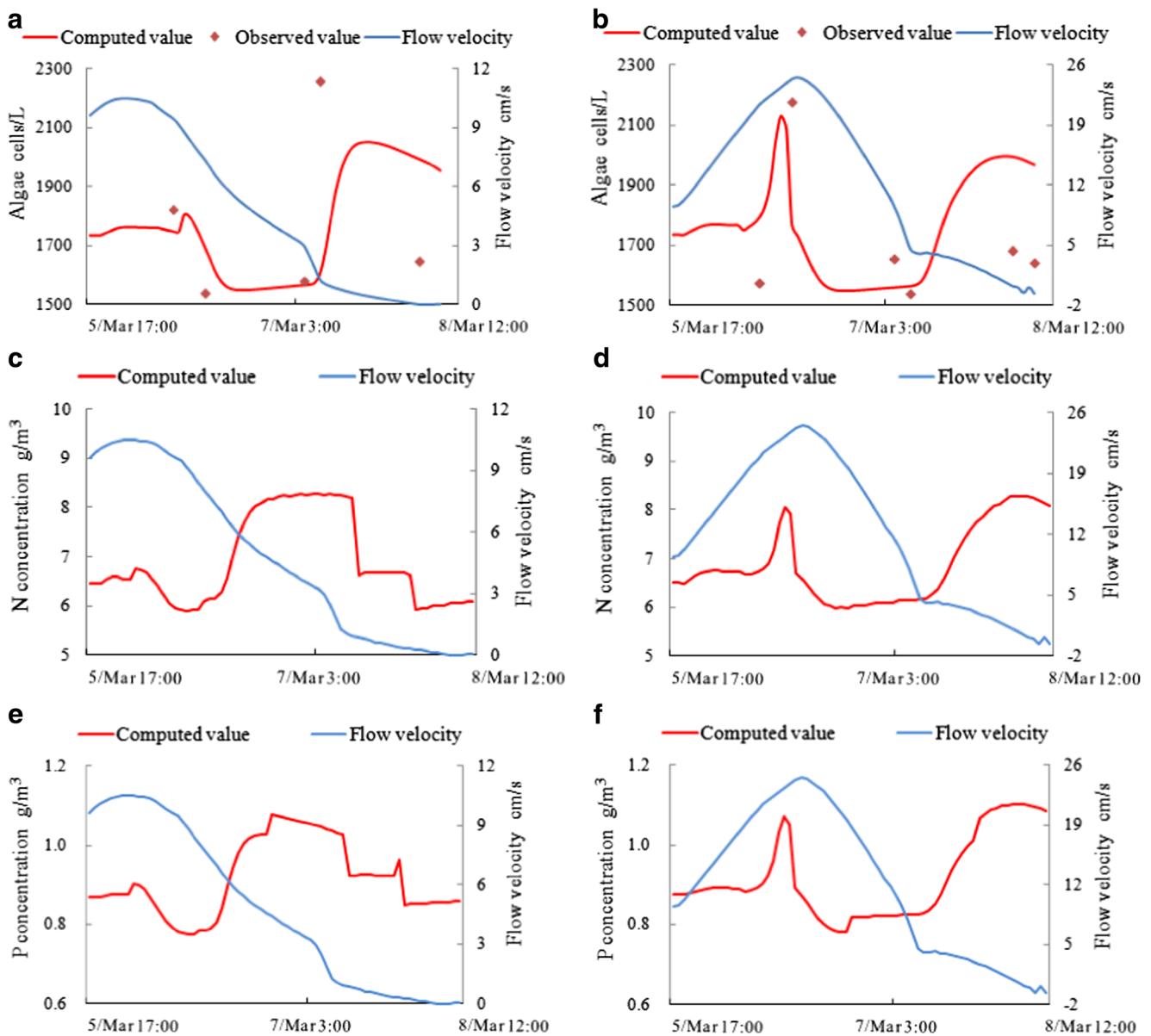


**Fig. 6** Trends in the concentrations of algae (a), N (c), and P (e) in the upper reaches of the sluice and the concentrations of algae (b), N (d), and P (f) in the lower reaches of the sluice

were not notable during this period, which indicated that the changes of the suspended pollutant concentrations were influenced not only by sedimentation but also by the pollutant concentrations associated with the incoming flow in the earlier stage. In the middle simulation stage, the flow velocity further decreased in front of the sluice because of decreased incoming flow discharge. Meanwhile, sedimentation increased, but resuspension was no longer notable. The degradation decreased, and absorption increased with decreased flow velocity. Therefore, the suspended pollutant concentrations notably decreased under the synthetic effects of these processes and the reduced rate of the suspended pollutants gradually decreased with further decrease in flow velocity. In the

later simulation stage, when the gate opening size was gradually decreasing until fully closed, the flow was blocked in front of the sluice, the water level rose higher, and all processes reached relatively stable conditions. Thus, the suspended pollutant concentrations slowly decreased or maintained. Overall, flow velocity is the most significant factor affecting the suspended pollutant concentration. If the flow velocity is higher than the critical velocity, the suspended pollutant concentrations are predicted to increase. If the flow velocity is lower than the critical velocity, the suspended pollutant concentrations are predicted to decrease. In addition, the suspended pollutant concentrations may also be influenced by water depth and temperature to a certain extent.

## Simulation results and analysis of alga concentrations

Based on the model mentioned above, changes in the amount of algae in the water in the upper and lower reaches of the sluice were simulated (Fig. 6).

Figure 6 shows that the amount of algae first increased and then decreased; this trend repeated later. Based on Fig. 6a, b, from 5:00 p.m. on March 5 to 9:00 a.m. on March 6, the amount of algae changed slowly in the upper and lower sections of the sluice because the incoming flow in the initial section did not reach the simulation section. Thus, the amount of algae was mainly affected by algal growth and death. From 9:00 a.m. on March 6 to 2:00 p.m. on March 6, the amount of algae in the upper and lower sections of the sluice increased, but in the upper reaches of the sluice did not significantly increase, and in the lower reaches of the sluice the opposite. This indicated that a small amount of algae accumulated in the upper section and many migrated with the flow of water to the lower section. In this stage, algae were mainly influenced by the migration of water flow. With the decreased water flow in the upstream sections and reduced flow velocity through the sluice gate, the algae increased rapidly both in the upstream and downstream sections. However, the increase was relatively rapid in the upstream section, but relatively slow in the downstream section, which indicated that change in the amount of algae was not only affected by the migration of water flow, but also by other effects. According to previous research (Cao 2008), algae have a maximum growth rate at a flow velocity of 30 cm/s. Based on the simulation results (Fig. 6), the flow velocity in the section in the upper reaches of the sluice decreased 1.87 cm/s after 12:00 p.m. on March 7, which is not suitable for algal growth. But the amount of algae, nonetheless, increased sharply with the decrease in the size of the gate opening. The reason why the algae increased might be the increase in the average value of alga density and the net increment of alga amount, which were caused by the delay in the upper reaches of the sluice and the accumulation in front of the gate with the migration of water.

In the lower reaches of the sluice, after 9:00 a.m. on March 7, the maximum flow velocity reached 10.76 cm/s, which reflected the least suitable conditions of flow velocity for algal growth. Algal growth was then in a declining stage, and the death rate was greater than the growth rate. Meanwhile, the flow volume of the sluice gate decreased, and the disturbance of the water body in the lower river reaches of the sluice decreased as well, leading to the weakening of water and nutrient absorption by algae and the alga suspension. Thus, the increase in sediments from the sedimentation of algae led to a slow increase in the amount of algae. When the sluice gate was closed, the disturbance of the water body was reduced both in the upper and in the lower river reaches, and the concentrations of nutrients decreased because of desorption and sedimentation. Then, the amount of algae

began to decrease due to the death rate being greater than the growth rate. The analysis revealed that the migration of water flow was notable with a large discharge volume before 12:00 p.m. on March 7. But the flow velocity, incoming discharge, and discharge volume of the sluice all decreased after 12:00 p.m. on March 7. The hydrodynamic conditions were no longer suitable for algal growth, and the increase in the alga amount was inhibited. Figure 6c–f shows that the N and P concentrations in algal cells changed with the amount of algae and that the extent of the change in N content is greater than that of P content in algal cells. Based on the simulated and measured values, the N/P ratio in water was about 33 in the upper river reaches and 37 in the lower river reaches, much higher than 16. To some extent, algal growth was limited by the concentration of phosphorus availability (Fisher et al. 1992), and the transformation of phosphorus from the algae to the dissolved pollutants was inhibited during this period.

## Conclusions

A multi-phase transformation model of pollutants in different phases was established in the SCRRs by the application of a number of theoretical methods. The Huaidian sluice area was taken as a study area to investigate changes of pollutant concentrations in different phases. The conclusions reached on the basis of this research are as follows:

1. The hydrological regimes were significantly affected by incoming flow and the opening size of the gate. Increased incoming flow rate or gate opening size led to increased release of matter from the suspended and sedimented pollutants and change in the amount of algae, which indirectly influenced other water quality transformation processes. Therefore, the dissolved and suspended pollutant concentrations increased, but those sediment pollutants decreased in the upper and lower reaches of the sluice. The results were opposite for decreased incoming flow rate or gate opening size.
2. Each reaction process exhibited strong and weak properties associated with change of the sluice operation mode in the SCRRs. When the sluice gate opening was decreased in size or fully closed, the flow velocity decreased in the section in front of or behind the sluice. Therefore, absorption and deposition increased, and the dissolved and suspended pollutants were transformed into the sediment pollutants at a relative high rate. When the sluice opening size increased, the high river flow caused the increase in desorption and resuspension rates, and the sedimented pollutants were transformed into dissolved and suspended pollutants at a relative high rate.
3. Exchange between the water body and external material was affected by the sluice operation mode. When the

sluice gate opening size was decreased or the sluice gate was closed, slow flow velocity would reduce aeration, leading to the weakening in nitrification, denitrification, and mineralization.

4. During the earlier period, the change in the amount of algae was mainly affected by the migration of water flow. During the later period, the change in the amount of algae in the section in the upper reaches of the sluice was mainly affected by the blocking of the sluice gate because the size of the gate opening decreased, whereas it was mainly affected by flow velocity, flow volume, and nutrient concentration in the lower reaches of the sluice.

**Funding information** The research was supported by the Natural Sciences Foundation of China (Nos. U1304509 and 51679218), the Outstanding Young Talent Research Fund of Zhengzhou University (No. 1521323001), and the Program for Science & Technology Innovation Talents in Universities of Henan Province (No. 17HASTIT031).

## References

- Ao XF, Wang XL, Song MR et al (2016) Three-dimensional water-quality simulation for river based on VOF method. *Trans Tianjin Univ* 22(5):426–433. <https://doi.org/10.1007/s12209-016-2732-9>
- Cao (2008) Study on the effect of hydrodynamic conditions on the occurrence and disappearance of cyanobacteria bloom. *Disaster Control Eng* 1:67–71
- Chen CY, Li K, Horne RN (2007) Experimental study of phase-transformation effects on relative permeabilities in fractures. *SPE Reserv Eval Eng* 10(05):514–526. <https://doi.org/10.2118/90233-PA>
- Chris JG, Joel RJ, Morris G et al (2016) The influence of sluice gate operation on the migratory behavior of Atlantic salmon *Salmo salar* (L.) smolts. *J Ecohydraulics* 1:90–101
- Cui YP, Ye F, Chen QW et al (2011) The variation trend of nutrient flux from Yangtze River and related impact on Yangtze estuary. *Asian Pacific Coasts* 2011:1046–1053
- Dou M, Zheng BQ, Zuo QT et al (2013) Identification of quantitative relation of ammonia-nitrogen concentration and main influence factors in the river reaches controlled by sluice. *J Hydraul Eng* 44:934–941
- Dou M, Li GQ, Li CY (2015) Quantitative relations between chemical oxygen demand concentration and its influence in the sluice-controlled river reaches of Shaying River, China. *Environ Monit Assess* 187:1–14
- Enner A, Marcelo C, Milton K et al (2016) Spatiotemporal total suspended matter estimation in Itumbiara reservoir with Landsat-8/OLI images. *Int J Cartogr* 2:148–165
- Fisher ER, Peale JW, Ammerman LB et al (1992) Nutrient limitation of phytoplankton in Chesapeake Bay. *Mar Ecol Prog Ser* 82:51–63. <https://doi.org/10.3354/meps082051>
- Frémion F, Courtin NA, Bordas F (2016) Impact of sediments resuspension on metal solubilization and water quality during recurrent reservoir sluicing management. *Sci Total Environ* 562:201–215. <https://doi.org/10.1016/j.scitotenv.2016.03.178>
- Gilmar PH, Marcos GN (2013) Reservoir design and operation: effects on aquatic biota—a case study of planktonic copepods. *Hydrobiologia* 707:187–198
- Guan JN, Liang DQ, NY W et al (2009) The methane hydrate formation and the resource estimate resulting from free gas migration in seeping seafloor hydrate stability zone. *J Asian Earth Sci* 36(4-5): 277–288. <https://doi.org/10.1016/j.jseae.2009.05.008>
- Hakanson L, Bryhn AC (2008) Modeling the foodweb in coastal areas: a case study of Ringkøbing Fjord, Denmark. *Ecol Res* 23(2):421–444. <https://doi.org/10.1007/s11284-007-0395-7>
- Hoff JT, Mackay D (1993) Partitioning of organic chemicals at the air-water interface in environmental systems. *Environ Sci Technol* 27(10):2174–2180. <https://doi.org/10.1021/es00047a026>
- Hu JT, Li SY (2009) Modeling the mass fluxes and transformations of nutrients in the Pearl River Delta, China. *J Mar Syst* 78:146–167
- Hu WW, Wang GX, Deng W et al (2008) The influence of dams on ecohydrological conditions in the Huaihe River basin, China. *Ecol Eng* 33:233–241
- Kondolf GM, Gao YX, Annandales GW et al (2014) Sustainable sediment management in reservoirs and regulated rivers: experiences from five continents. *Earth's Future* 2(5):256–280. <https://doi.org/10.1002/2013EF000184>
- Koutsos TM, Dimopoulos GC, Mamolos AP (2010) Spatial evaluation model for assessing ad mapping impacts on threatened species in regions adjacent to Natura 2000 sites due to dam construction. *Ecol Eng* 36(8):1017–1027. <https://doi.org/10.1016/j.ecoleng.2010.04.011>
- Lebo ME, Sharp JH (1992) Modeling phosphorus cycling in a well-mixed coastal plain estuary. *Estuar Coast Shelf Sci* 35:235–252
- Li QF, Yu MX, Zhao JH et al (2012) Impact of the Three Gorges reservoir operation on downstream ecological water requirements. *Hydrol Res* 43(1-2):48–53. <https://doi.org/10.2166/nh.2011.121>
- Li RH, Pan W, Guo JC et al (2014) Studies on kinetics of water quality factors to establish water transparency model in Neijiang River, China. *J Environ Biol* 35(3):513–519
- Liu C, Li XW, Wei HP et al (2003) Numerical simulation of the hydrodynamics and sewage diffusion in the Changjiang River Estuary. *Oceanologia et Limnologia Sinica* 34:474–483
- Liu HB, Li YH, Leng F et al (2016) Stage variation of phytoplankton and environmental factors in a large drinking water reservoir: from construction to full operation. *Water Air Soil Pollut* 227:1–12
- Lothar P, Klaus P (2008) Suspended matter elimination in a pre-dam with discharge dependent storage level regulation. *Limnologia-Ecology and Management of Inland Waters* 38:388–399
- Ludovic C, Gilles B (2012) Experimental and numerical investigation of flow under sluice gates. *J Hydraul Eng* 138:367–386
- Mevlut SA, Mehmet SK, Ahmet AO (2009) Experimental and numerical modeling of a sluice gate flow. *J Hydraul Res* 47:167–176
- Michalski R, Jabłońska CM, Szopa S et al (2016) Variability in different antimony, arsenic and chromium species in waters and bottom sediments of three water reservoirs in Upper Silesia (Poland): a comparative study. *Int J Environ Anal Chem* 96(7):682–693. <https://doi.org/10.1080/03067319.2016.1180382>
- Molisani BH, Barroso HS et al (2013) The influence of castanhão reservoir on nutrient and suspended matter transport during rainy season in the ephemeral Jaguaribe river (CE, Brazil) Influência do açude Castanhão no transporte de nutrientes e materiais em suspensão durante a estação chuvosa no intermitente rio Jaguaribe (CE, Brasil). *Braz J Biol* 73(1):115–123
- Petkovsek G, Roca M (2014) Impact of reservoir operation on sediment deposition. *Proceedings of ICE: Water Management* 167:577–584
- Tappin AD, Harris JRW, Uncles RJ (2003) The fluxes and transformations of suspended particles, carbon and nitrogen in the Humber estuarine system (UK) from 1994 to 1996: results from an integrated observation and modelling study. *Sci Total Environ* 314-316:665–713. [https://doi.org/10.1016/S0048-9697\(03\)00078-0](https://doi.org/10.1016/S0048-9697(03)00078-0)
- Walling DE, Fang D (2003) Recent trends in the suspended sediment loads of the world's rivers. *Glob Planet Chang* 39(1-2):111–126. [https://doi.org/10.1016/S0921-8181\(03\)00020-1](https://doi.org/10.1016/S0921-8181(03)00020-1)
- Wang B, SQ L, Lin WQ et al (2016a) Water quality model with multiform of N/P transport and transformation in the Yangtze River Estuary.

- Journal of Hydrodynamics, Ser B 28(3):423–430. [https://doi.org/10.1016/S1001-6058\(16\)60645-5](https://doi.org/10.1016/S1001-6058(16)60645-5)
- Wang BY, Yan DCH, Wen AB et al (2016b) Influencing factors of sediment deposition and their spatial variability in riparian zone of the Three Gorges Reservoir, China. *J Mt Sci* 13(8):1387–1396. <https://doi.org/10.1007/s11629-015-3806-1>
- Wang JH, Xiao WH, Wang H, Chai ZK, Niu CW, Li W (2013) Integrated simulation and assessment of water quantity and quality for a river under changing environmental conditions. *Chin Sci Bull* 58(27):3340–3347. <https://doi.org/10.1007/s11434-012-5622-0>
- Wang P, Hu B, Wang C (2015) Phosphorus adsorption and sedimentation by suspended sediments from Zhushan Bay, Taihu Lake. *Environ Sci Pollut Res* 22(9):6559–6569. <https://doi.org/10.1007/s11356-015-4114-6>
- Xia J, Dou M, Zhang H (2001) Dynamic model of eutrophication in Hanjiang River. *Chongqing Environmental Science* 1:20–24
- Yang Y, Wu XY, Guan WB (2012) Modeling study on water ecology in Changjiang River Estuary and its adjacent areas during dry season. *J Marine Sci* 30:16–28
- Zhang XK, Wan A, Wang H et al (2016) The overgrowth of *Zizania latifolia* in a subtropical floodplain lake: changes in its distribution and possible water level control measures. *Ecol Eng* 89:114–120. <https://doi.org/10.1016/j.ecoleng.2016.01.069>
- Zhang Y, Dou M, Yu D (2015a) Identification of the key factors affecting water quality concentration in the river reach controlled by sluice based on statistical methods. *Environ Sci Technol* 38:61–67
- Zhang YY, Zh XY, Sh QX et al (2015b) Assessing temporal and spatial alterations of regimes in the regulated Huai River Basin, China. *J Hydrol* 529:384–397. <https://doi.org/10.1016/j.jhydrol.2015.08.001>
- Xi L, Chen P, Deng HY et al (2014) Study on pollution load of livestock industry in Shaying River Watershed of Hehan. *J Henan Agric Sci* 38:135–140
- Chen YZ, Chen ZF, Ma JH et al (2016) Effects of soil-nitrate nitrogen on the nitrate accumulation in groundwater and vegetables in a typical high cancer incidence area of Shaying River basin. *Acta Sci Circumst* 36:990–998
- Hao SN, Peng WQ, Wu WQ et al (2014) Research on spatial distribution of non-point source pollution load in Shaying River Basin. *Yangtze River* 45:6–10